Phase Transitions
Publication details, including instructions for authors and subscription information:
http://www.tandfonline.com/loi/gpht20

A study on graphitisation acceleration during annealing of martensitic hypereutectoid steel

S.A. Rounaghi [a] & A.R. Kiani-Rashid [a]
[a] Department of Materials Engineering, Ferdowsi University of Mashhad, Mashhad, Iran

Available online: 22 Aug 2011

To cite this article: S.A. Rounaghi & A.R. Kiani-Rashid (2011): A study on graphitisation acceleration during annealing of martensitic hypereutectoid steel, Phase Transitions, 84:11-12, 981-991

To link to this article: http://dx.doi.org/10.1080/01411594.2011.563153

Phase Transitions
Vol. 84, Nos. 11–12, November–December 2011, 981–991

Taylor & Francis
Taylor & Francis Group

A study on graphitisation acceleration during annealing of martensitic hypereutectoid steel

S.A. Rounaghi* and A.R. Kiani-Rashid

Department of Materials Engineering, Ferdowsi University of Mashhad, Mashhad, Iran

(*Received 31 December 2010; final version received 11 February 2011*)

In this experimental study, the influence of primary martensitic structure on acceleration of graphitisation process in hypereutectoid steels during subsequent heat treatment cycle was investigated by using optical microscopy and scanning electron microscopy. Then, the results have been compared with prior pearlitic and spheroidized structures. Dilatometric experimental results demonstrated the following graphitisation process from Johnson–Mehl–Avrami equation for steels with a prior martensitic structure. The Avrami exponent was determined about 1.4 that indicates a diffusion-controlled nucleation and growth mechanism in this kind of phase transformation.

Keywords: steel; graphitisation; martensite; transformation

1. Introduction

Graphitisation in steels can improve the machinability and cold-work-ability [1,2]. For the first time, Sueyoshi et al. [3] attempted to improve the machinability and forge-ability by changing the microstructure of medium carbon steel to a soft ferrite structure made by dispersing graphite particles. Later, Katayama and Toda [4] showed that the tool life during machining graphitic medium carbon steels can be increased 2–7 times compared with conventional free cutting steels and cemented carbide insert. The same results have been reported by Iwamoto and Murakami [5]; they also achieved higher fatigue strength after quenching and tempering in comparison with leaded steels and offered graphitic steels can be substituted for this family of steel which have distractive bioenvironmental effects.

Despite the above-mentioned ones, one of the major disadvantages which can be attributed to the graphitic steels is the very long annealing time. This is due to the presence of carbide stabilizer elements such as chromium and manganese in commercial steels which reduce graphitisation driving force [6], another factor which can reduce the graphitisation driving force is low percentage of carbon as the best graphite stabilizer elements in steels in comparison to conventional cast irons [7].

To overcome this problem, some authors tried to reduce graphitisation time by adding graphitiser elements such as silicon to the melt during steel making [8]. Moreover, He et al. [8] and Banerjee and Venugopalan [9] demonstrated some alloying elements such as Al and

*Corresponding author. Email: s.a.rounaghi@gmail.com

ISSN 0141–1594 print/ISSN 1029–0338 online

http://dx.doi.org/10.1080/01411594.2011.563153
http://www.tandfonline.com

B can form AlN and BN compounds in steel, which can be considered as an excellent nucleus for graphite nodules and also accelerate the graphite nucleation. Prior steel treatment can also affect the graphitisation process. In this regard, cold working of steel can decrease the subsequent annealing time remarkably [10]. Also it has been demonstrated that kinetic of graphite phase formation after cold rolling is in good agreement with the Johnson–Mehl–Avrami equation [10]. He et al. [6,11] studied the graphitisation process in medium carbon alloyed steels from prior martensitic and bainitic structures and could reduce the transformation time to 2 h. Rosen and Taub [12] performed similar tests on eutectoid steels. They investigated the graphitisation transformation from different structures in the temperature range between 575°C and 700°C. Their results confirm that the transformation follows from the Johnson–Mehl–Avrami equation and shortest time for graphitisation completion is measured for prior martensitic structure [12].

Although martensitic structure is known as a good choice for acceleration graphitisation process, the effect of quenching media and martensitic structure on subsequent annealing treatment is still unknown and less mentioned by other authors. Also, a comprehensive study of microstructure evolution during the transformation assisted by dilatometric experiments has not been investigated yet. So, a systematic study on the accelerating factors from a kinetic viewpoint can help to reduce the industrial processing time and makes manufacturing process more efficient. In this respect, graphitisation behavior has been studied from different prior structures such as pearlitic, martensitic, and spheroidized and the parameters which can accelerate the process from martensitic structures have been investigated.

2. Experimental procedure

The steel used in this research is a low alloy hypereutectoid grade with the commercial name of CK100 and its chemical composition is given in Table 1. This low alloy steel was selected to reduce the effect of alloying elements on kinetic and thermodynamic of phase transformation. The spheroidizing treatment was carried out at 770°C for 4 h, then specimens were cooled to 660°C at the rate of 6°C per hour and held at this temperature for 4 h followed by cooling in air. In order to distinguish the specimens subjected to varied heat treatment schedules, they were identified with code numbers, as described in Table 1.

For dilatometric analysis, round test pieces of 4 mm diameter and 16 mm length were machined from the spheroidized (as received) steel. Dilatometric analysis was conducted by means of a Linseis machine model 2171. Martensitic structure was performed by austenitizing dilatometric specimens at 900°C for 20 min in electrical furnace and subsequent quenching to room temperature in two different environments. In another word, in order to investigate the effect of quenching media, quenching was carried out in water and oil. Then, the dilatometric study was performed isothermally at 670°C on these specimens. For more confidence, each test was repeated two times. The heating rate of

Table 1. Chemical composition of CK100 steel.

Steel	C	Si	S	P	Mn	Ni	Cr	Mo	Cu	Al
CK100	0.949	0.213	0.012	0.017	0.339	0.047	0.061	0.008	0.076	0.017

Note: Weight percent.

Table 2. Heat treatment cycles applied on experimented specimens.

Specimen	Heat treatment cycle
1	Spheroidized (as received)
2	900°C, 20 min → air cooled (pearlitic/cementitic steel)
3 (Dilatometric test)	900°C, 20 min → water quenched → graphitised at 670°C
4 (Dilatometric test)	900°C, 20 min → oil quenched → graphitised at 670°C
5 (Dilatometric test)	900°C, 20 min → water quenched → graphitised at 670°C for 6.5 h
6 (Dilatometric test)	900°C, 20 min → water quenched → graphitised at 670°C for 12 h
7 (Dilatometric test)	900°C, 20 min → water quenched → graphitised at 670°C for 60 h
8	900°C, 20 min → air cooled → graphitised at 670°C for 110 h
9	Spheroidized → graphitised at 670°C for 110 h

dilatometric specimens from room temperature to 670°C was considered 100°C min^{-1}. The dilatometric test was carried out in different times (specimens No. 5, 6, and 7) and after that, the specimen was air cooled and prepared for microstructure study. Specimen No. 5 was extracted from the first changes after 6.5 h in the dilatometric specimen. Also, data analysis on dilatometric results was performed by the Origin 7.5 graphing software (Table 2).

To compare the graphitisation from martensitic structure with other ones, the process was investigated by using two different structures, i.e., the spheroidized steel (specimen No. 1) and the pearlitic/cementitic steel. Also, the dimensions of these specimens were selected to be similar to dilatometric specimens. The pearlitic/cementitic steel was prepared by austenitizing the spheroidized steel at 900°C for 20 min and then cooling the specimens outside the furnace in air. Also, the graphitisation temperature for all structures was considered at 670°C similar as martensitic one.

In order to prevent decarburization of specimens during austenitizing treatment and during the prolonged annealing, the surface of specimens was covered with an anti-carburizing layer called as Carbostop. Moreover, pearlitic/cementitic and spheroidized specimens were put in a container having cast iron filings to prevent decarburization.

In order to perform metallographic investigation of the microstructure, all samples were sectioned and optical microscopic (OM) and scanning electron microscopic (SEM) micrographs were produced from their central regions after conventional surface grinding and polishing followed by etching in 2% Nital.

For some microstructural study of specimens, SEM micrographs and EDX analysis were prepared in Razi Metallurgy Research Center using TESCAN machine and for preparing other images, the SEM model 1450 VP made by Zeis Germany from the Central Laboratory of Ferdowsi University of Mashhad was used.

3. Results and discussions

3.1. *Dilatometric studies*

Figure 1 shows the dilatometric diagram of graphitisation transformation from martensitic structure for different quenching media (specimens No. 3 and 4). It can be seen that the

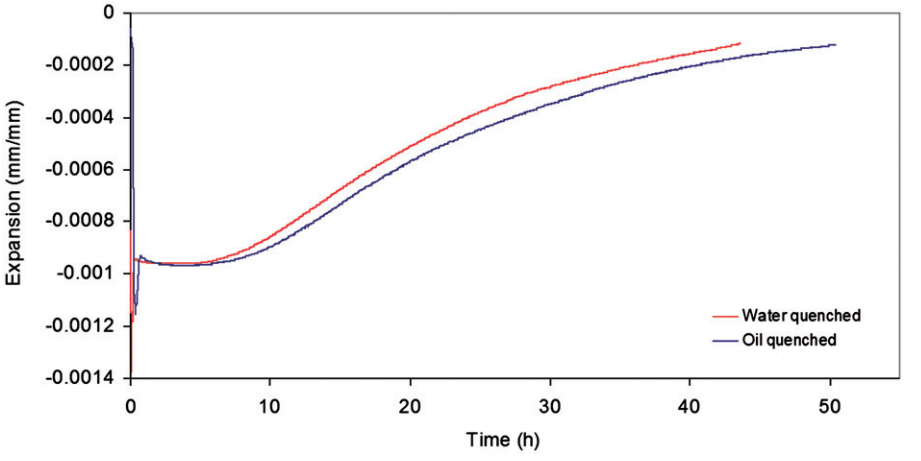

Figure 1. Graphitisation dilatometric diagram related to water quenched and oil quenched specimens (specimens No. 3 and 4).

trend of the curves follows Johnson–Mehl–Avrami equation [13]:

$$X = 1 - \exp(-Kt_{\mathrm{Tr}}^{n}) \tag{1}$$

where

$$t_{\mathrm{Tr}} = t_{\mathrm{t}} - t_{\mathrm{i}} \tag{2}$$

and X is the volume fraction of the phase transition, t_{Tr} the Transformation time, t_{t} the total time, t_{i} the incubation time, K the temperature-dependent coefficient, and n the Avrami exponent.

Time in Equation (1) must be considered as transformation time (t_{Tr}), not overall time (t_{t}), which has been calculated by dilatometer in Figure 1. So, as explained by Equation (2), the time elapsed before that graphitisation transformation can be detectable by dilatometer (t_{i}) must be subtracted from the t_{t}.

To find an equation which fits the dilatometric data best, we first applied Equation (2) to calculate transformation time (t_{Tr}); then, by choosing growth functions from Origin formula database, the results were automatically analyzed and fitted to Avrami equation and proper values for Avrami parameters were determined as follows:

For water quenched specimen,

$$X = 1 - \exp(-5.29 \times 10^{-5} t_{\mathrm{Tr}}^{1.404}) \tag{3}$$

and for oil quenched specimen,

$$X = 1 - \exp(-2.49 \times 10^{-5} t_{\mathrm{Tr}}^{1.459}) \tag{4}$$

By plotting Equations (3) and (4), it has been demonstrated that these equations are in good agreement with experimental data; so, by extrapolating these equations, one can calculate the end of transformation time (Figure 2). The determined values for n, i.e., 1.4, explain a diffusion-controlled nucleation and growth kinetics which illustrate that nucleation takes place on grain boundaries and dislocations [14,15].

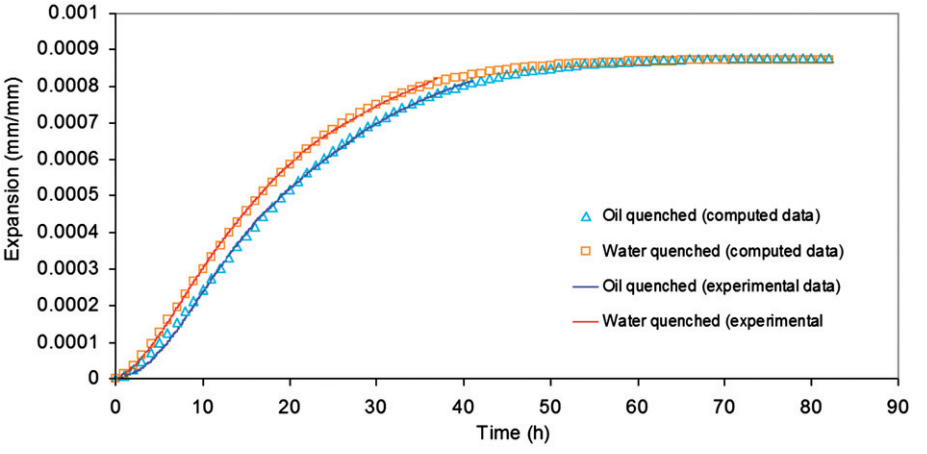

Figure 2. Experimental and computed curves which have been extracted from experimental dilatometric data and Origin software, respectively.

Table 3. Effect of quenching media on graphitisation time.

Quenching media	$t_{0.05}$ (h)	$t_{0.5}$ (h)	$t_{0.95}$ (h)
Water	4.8	18.9	45.1
Oil	5.1	21.6	50.8

Another important point which can be concluded from Figures 1 and 2 is the effect of quenching media on graphitisation kinetic. Table 3, which is extracted from the dilatometric data, shows the effect of quenching media on the relevant time which is needed for different graphitized volume fractions. As it can be seen, the time associated with each stage reduces for the water quenched specimen in comparison with the oil quenched one. These remarkable changes can be attributed to variation of the number of crystal defects, especially dislocation densities during different cooling rate. In this respect, Ohmori and Tamura [16] have supposed that crystal defects such as dislocations are preferred regions for carbon segregation in the martensite. A similar result also can be concluded from the Avrami exponent in Equations (3) and (4) which supposes that dislocations and grain boundaries are preferred sites for graphite nucleation. So, higher cooling rate of water compared to oil can increase dislocation densities in the water quenched specimen than in the oil quenched one, which leads to increased nucleation sites for graphite particles in the first stage of annealing and can be detected more rapidly by dilatometer. In confirmation of this theory, at the same time of annealing, significant reduction in the number of graphite particles was observed in the oil quenched specimen in comparison with the water quenched one. The effect of this reduction in the number of graphite nucleus can postpone and limit graphite growth in subsequent stages. In this respect, the highest difference between graphitisation time in these specimens can be concluded at final stages ($t_{0.95}$) of annealing (about 5.7 h). On the other hand, Avrami exponent ($n = 1.4$) explains that diffusion is a dominant parameter on graphite nucleation

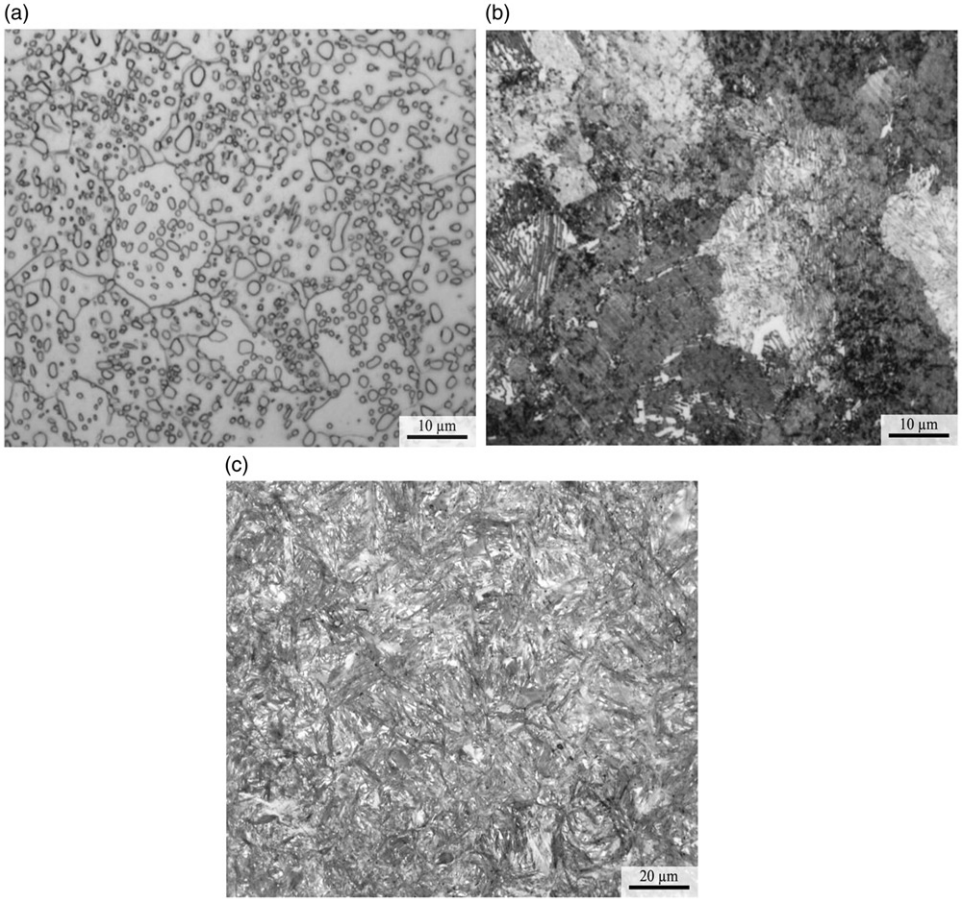

Figure 3. Primary steel structures (a) spheroidized (as received), (b) pearlitic/cementitic, and (c) martensitic.

and grows, which is consistent with finding of other researchers [12], higher amounts of dislocations as carbon diffusion paths in water quenched specimen can accelerate graphitisation transformation in this specimen.

3.2. *Microstructural studies*

Figure 3 illustrates all primary structures before graphitisation. The microstructure of spheroidized steel (specimen No. 1) includes ferrite and spherical carbides (Figure 3a) while the martensitic structure containing some retained austenite (bright regions) can be seen in water quenched specimen (Figure 3c).

Figure 4(a) and (b) illustrates the graphitized structure from the water quenched specimen (specimen No. 7) after 60 h annealing at 670°C. Although such long annealing time is not justified in terms of industrial manufacturing, even after short annealing time, significant changes in steel properties can be reached [9,17]. Also, graphitisation annealing can be considered as an alternative for spheroidizing annealing which is a prolonged

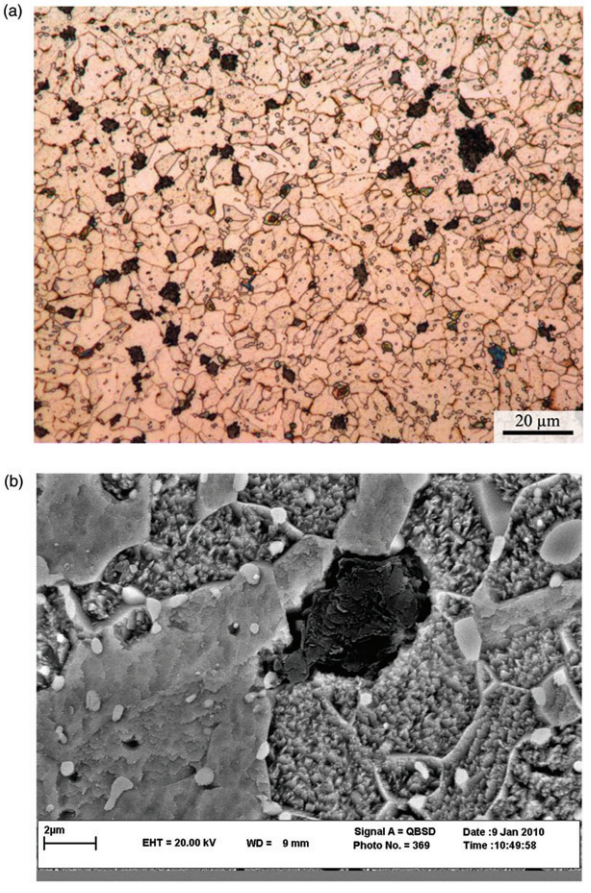

Figure 4. (a) Micrograph of graphitized steel (related to specimen No. 7) after annealing at 670°C for 60 h from prior martensitic structure; (b) SEM micrograph from a graphite particle in the same specimen.

annealing process that is carried out on high carbon steels at temperatures above 700°C to improve their machinability and cold forgeability [18].

As illustrated in Figure 4(a) and (b), graphitized microstructure consisted of ferritic matrix, graphite particles, and retained carbides. The details of microstructure and morphology of graphite particles have been described elsewhere [19,20]. The same structures also are observed in pearlitic/cementitic and spheroidized specimens (specimens No. 8 and 9) after annealing at 670°C for 110 h (Figure 5a and b). However, by investigating the graphitisation behavior of these specimens by means of the optical microscopy after 75 h at 670°C, no graphite particle was observed in the structures.

By analyzing the optical microscope micrographs, the surface area percent of graphite in specimens No. 7, 8, and 9 was calculated as 3.41, 0.14, and 0.15, respectively, which show the profound effect of martensite structure, even at shorter annealing time (60 h), on increasing amounts of formed graphite in comparison with other structures. These evidence of reductions in graphitisation time and graphite quantities make martensitic structure more favorable for manufacturing process. Figure 5(a) and (b) also illustrates

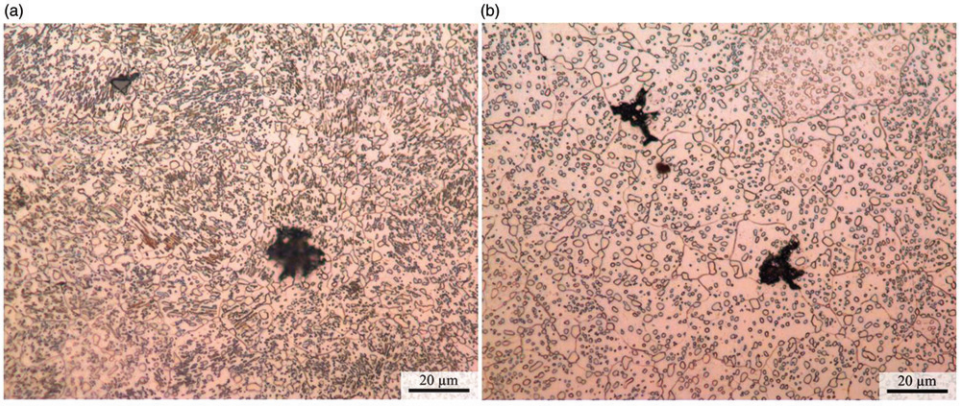

Figure 5. Graphitisation from non-martensitic structures: (a) micrograph of graphitized steel after annealing at 670°C for 110 h from prior pearlitic/cementitic structure related to specimen No. 8; (b) micrograph of graphitized steel after annealing at 670°C for 110 h from prior spheroidized structure (related to specimen No. 9).

that graphite particles have a larger size, uneven distribution and limited number compared to specimen No. 7 (Figure 4). One parameter which can explain these differences is higher crystal defects such as dislocations in the martensitic structure than other ones that is due to higher cooling rate of this structure. So as discussed above, this can cause increased diffusion coefficient and carbon precipitation regions and subsequently increases graphitisation rate.

By investigating the microstructures of graphitized specimens (Figure 4a and b), it is observed that most of the graphite particles are formed on ferrite grain boundaries. It may be due to significant difference between graphite and ferrite lattices, so ferrite grain boundaries can be known as good regions for graphite particles nucleation. This also confirms the nucleation of graphite particles on grain boundaries which was concluded from Avrami exponent ($n = 1.4$). On the other hand, as mentioned in previous section, kinetic of graphitisation is controlled by diffusion so the grain boundary diffusion can play a major role on growth of graphite nucleus. Moreover, it must be indicated that the size of ferrite grains in treated martensite even after annealing for 60 h (Figure 4a and b) is smaller than the spheroidized steel (Figure 3a). Therefore, another accelerating factor for graphitisation from martensite structure is the formation of fine grained ferrite during tempering [21], and the increase of grain boundary surfaces as carbon diffusion paths and nucleation sites for graphite particles. Similar effect of small ferrite grain size on acceleration and enhancement of graphite formation has been reported in semi-solid processing of ultrahigh carbon steels [17].

To study the microstructure in the first stage of graphitisation from martensitic structure, specimen No. 5 has been prepared. The presence of very small graphite particles in this specimen has been confirmed by using SEM and conducting EDX analysis (Figure 6b and c). By comparing Figure 6(a) and (b) with Figure 5(a) and (b), it may be concluded that partial spheroidizing of carbides precedes the graphitisation from all three structures. Such competition between spheroidizing and graphitisation process also has been reported by other authors [17,22]. So, it seems these globular carbide particles formed in all structures have major effect on graphitisation kinetics. In this context, the size of carbide particles in martensitic structure (specimen No. 5) is smaller than other ones

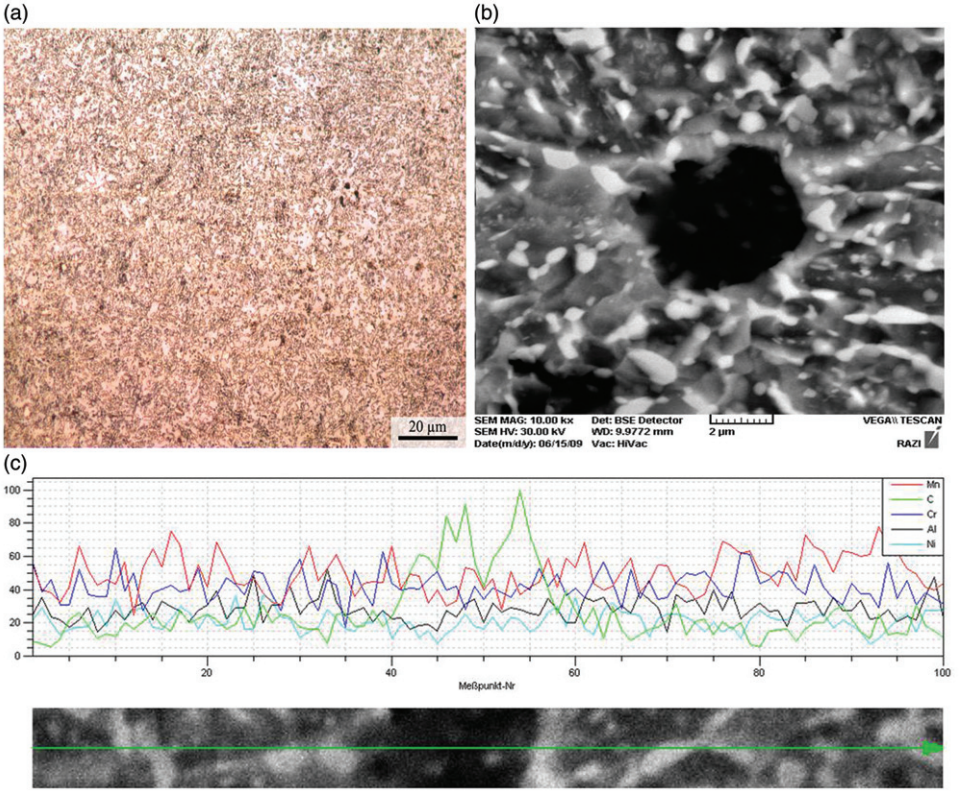

Figure 6. Structure of dilatometric specimen after initial length change due to graphitisation transformation after annealing at 670°C for 6.5 h (related to specimen No. 5). (a) OM micrograph form specimen microstructure, (b) SEM micrograph from the same specimen, and (c) EDX and line scan analyse of a dispatched graphite particle and its around regions in specimen No. 5.

(specimens No. 8 and 9), which can increase the cementite/ferrite interfaces and therefore influences the surface of transformation for graphitisation. This phenomenon accelerates the overall reaction rate in the aforementioned structure. On the other hand, the intermetallic compounds (such as AlN) and cementite particles can perform as nucleus for graphite nodules [6,9]. Especially, He et al. [6,8] showed amorphous carbon rich part formed on cementite particles during annealing martensite structure are preferred regions for graphite nucleus formation. Since all specimens are performed from one composition (Table 1) and steel has not been alloyed, it can be assumed that the role of intermetallic compounds as nucleus for graphite particles is negligible for all structures. Therefore, the role of carbide particles becomes more evident. Hence, as concluded by comparison of Figure 4a with Figure 6a and b, high number of density of very fine cementite particles in martensitic structure than the other ones can be observed, which act as graphite nucleus and subsequently increase the rate of graphitisation. This difference in the number of graphite particles can be observed even in the martensitic specimen during the initial graphitisation periods (Figure 7). Finally, by taking advantage of martensitic structure, significant reduction on the graphitisation time and a noticeable increase in the quantity of graphite particles can be achieved. Also, as mentioned, the addition of some graphitiser

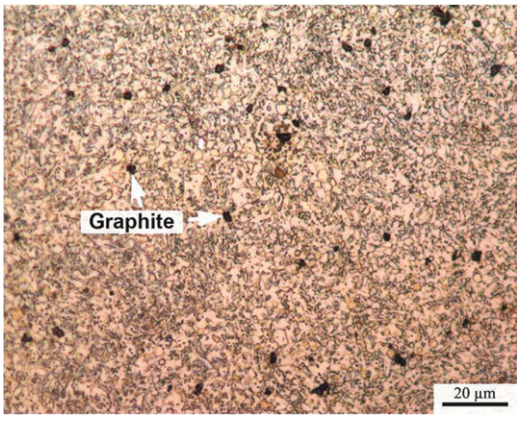

Figure 7. Micrograph of graphitised steel after annealing at 670°C for 12 h from prior martensitic structure (related to specimen No. 6).

elements can reduce this phase transformation significantly and make the process more favorable from the viewpoint of industrial processing [8].

4. Conclusions

The graphitisation phase transformation from various microstructures was studied by use of dilatometric analysis and microscopic investigations. By analyzing the recorded dilatometric data, a fitting process was performed to verify the behavior which is convenient to use the Johnson–Mehl–Avrami equation. The Avrami exponent indicated that transformation kinetic is controlled by diffusion-controlled nucleation and growth mechanism.

According to Avrami exponent and microscopic observations, it has been deduced that formation of fine ferrite grains, very small and nearly spherical cementite particles and high dislocations density during annealing martensitic structure can be considered as major parameters, which can accelerate graphitisation process from this structure.

Acknowledgments

The authors would like to express their gratitude from technicians of Metallurgical and Material Science Department of Ferdowsi University of Mashhad for their assistance. The authors also appreciate Dr Ahad Zabet and Part Sazan Co. for preparing some of the optical microscopy images. Moreover, the authors thank Mr Payam Shayesteh and Mr Ghasem Isa Abadi Bozchelouie for performing some experimental work.

References

[1] N.E. Luiz and Á.R. Machado, *Development trends and review of free-machining steels*, Proc. IME B. J. Eng. Manufact. 222(2) (2008), pp. 347–360.

[2] K. He and D.V. Edmonds, *A potential graphitisation route to improved machinability of carbon steels*, International Conference on New Developments in Long and Forged Products: Metallurgy and Applications, Rio de Janeiro, 2006, pp. 49–56.

[3] H. Sueyoshi, T. Ohsige, K. Suenaga, and R. Tanaka, *Machinability of hypo-eutectoid graphitic steel*, J. Japan Inst. Metals 52(12) (1988), p. 1285.
[4] S. Katayama and M. Toda, *Machinability of medium carbon graphitic steel*, J. Mater. Process. Technol. 62 (1996), pp. 358–362.
[5] T. Iwamoto and T. Murakami, *Bar and wire steels for gears and valves of automobiles-eco-friendly free cutting steel without lead addition*, JFE GIHO 4 (2004), pp. 64–69.
[6] K. He, A. Brown, R. Brydson, and D.V. Edmonds, *An EFTEM study of the dissolution of cementite during the graphitisation annealing of a quenched medium carbon steel*, J. Phys. Conf. 26(1) (2006), pp. 111–114.
[7] M. Tisza, *Physical Metallurgy for Engineers*, ASM International, Materials Park, OH, 2001, p. 338.
[8] K. He, H.R. Daniels, A. Brown, R. Brydson, and D.V. Edmonds, *An electron microscopic study of spheroidal graphite nodules formed in a medium-carbon steel by annealing*, Acta Mater. 55 (2007), pp. 2919–2927.
[9] K. Banerjee and T. Venugopalan, *Development of hypoeutectoid graphitic steel for wires*, Mater. Sci. Tech. 24 (2008), pp. 1174–1178.
[10] M.A. Neri, R. Colás, and S. Valtierra, *Effect of deformation on graphitisation kinetics in high carbon steels*, J. Mater. Process. Technol. 83 (1998), pp. 142–150.
[11] K. He, A. Brown, R. Brydson, and D.V. Edmonds, *Analytical electron microscope study of the dissolution of the Fe_3C iron carbide phase (cementite) during a graphitisation anneal of carbon steel*, J. Mater. Sci. 41 (2006), pp. 5235–5241.
[12] A. Rosen and A. Taub, *The kinetics of graphitisation in steel at subcritical temperatures*, Acta Metall. 10 (1962), pp. 501–509.
[13] M. Avrami, *Kinetics of phase change 2: Transformation-time relations for random distribution of nuclei*, J. Chem. Phys. 8 (1940), pp. 212–224.
[14] K.A. Jackson, *Kinetic Processes: Crystal Growth, Diffusion, and Phase Transitions in Materials*, 2nd ed., Wiley-VCH, Weinheim, 2010, pp. 205–211.
[15] J.W. Christian, *The theory of phase transformations in metals and alloys*, 2nd ed., Pergamon, Oxford, 1975, pp. 538–546.
[16] Y. Ohmori and I. Tamura, *Interpretation of the carbon redistribution process during aging of high carbon martensite*, Metall. Trans. A 23 A (1992), pp. 2147–2158.
[17] M. Ramadan, M. Takita, H. Nomurab, and N. El-Bagoury, *Semi-solid processing of ultrahigh-carbon steel castings*, Mater. Sci. Eng. A 430 (2006), pp. 285–291.
[18] G.E. Totten, *Steel Heat Treatment: Metallurgy and Technologies*, CRC Press, USA, 2007.
[19] S.A. Rounaghi, P. Shayesteh, and A.R. Kiani-Rashid, *Evolution of graphite phase morphology during graphitisation process in hypereutectoid steels*, Int. Foundry Res./Giessereiforschung 62(3) (2010), pp. 2–6.
[20] S.A. Rounaghi, P. Shayesteh, and A.R. Kiani-Rashid, *Microstructural study in graphitised hypereutectoid cast and commercial steels*, Mater Sci Tech Ser. 27 (2011), pp. 631–636.
[21] T. Maki, S. Morito, and T. Furuhara, *The change in matrix structure during tempering of lath martensite in Fe–C alloys*, 19th ASM Heat Treating Society Conference and Exposition including Steel Heat Treating in the New Millenium, Cincinnati, OH, 1999, pp. 631–637.
[22] L.E. Samuels, *Light Optical Microscopy of Carbon Steels*, ASM, Metals Park, OH, 1999.